

Remote Raman spectroscopy of explosive precursors

Emanuela Gallo[✉],* Luca Cantu, and Frank Duschek[✉]

German Aerospace Center, Institute of Technical Physics, Hardthausen, Germany

Abstract. Deep ultraviolet Raman spectroscopy measurements have been performed at the German Aerospace Center (DLR) with the aim of detecting traces (μg range) of explosive precursors. In this study, a backscattering Raman system was setup and optimized to detect urea, sodium perchlorate, ammonium nitrate, and sodium nitrate at a 60-cm short-range remote detection. The sample was tested at 264-nm ultraviolet laser excitation wavelength to experimentally observe any possible trace over textiles samples. For each colored sample textile, Raman spectra were acquired and no background fluorescence interference was observed at this laser excitation wavelength. Detection limits and system sensitivity with an acquisition time up to 3 s for microgram traces are presented. © The Authors. Published by SPIE under a Creative Commons Attribution 4.0 Unported License. Distribution or reproduction of this work in whole or in part requires full attribution of the original publication, including its DOI. [DOI: [10.1117/1.OE.60.8.084108](https://doi.org/10.1117/1.OE.60.8.084108)]

Keywords: Raman spectroscopy; explosive precursors; remote detection.

Paper 20210501 received May 11, 2021; accepted for publication Aug. 16, 2021; published online Aug. 27, 2021.

1 Introduction

Remote laser-based techniques are useful to detect harmful substances (such as vapors and particles from explosives or surface traces such as a fingerprint residue) without requiring direct contact from the operator. A potential warning at a safe distance from the identification site is wanted to both save the life of the personnel investigating a contaminated area and avoid directly damaging the detection required equipment.¹ Among many available laser-based techniques, Raman spectroscopy is a powerful tool to detect and uniquely identify unknown substances. It is non-destructive and highly selective²⁻⁶ while other techniques such as infrared spectroscopy suffers more on the background surface (surface reflectivity and roughness) and sample size (thickness), which affects peak positions and intensities,⁷ or laser-induced fluorescence, which is highly sensitive but poorly selective.⁷ Spectroscopic detection of explosive traces and their precursors is a very important topic for homeland security applications to reduce the threat of improvised explosive devices (IED). A precursor is a common material easily available on the markets, such as fertilizers, food preservatives, solvents for cleaning agents, fuels, and pyrotechnic kits, which can be turned into an explosive with minimal effort by mixing or blending with other chemicals or by simple chemical processing (see EU regulation No. 98/2013, Ref. 8). Hence, it is critical to be able to detect those chemicals before a detonation happens. Often, after handling, traces of the chemical compounds easily stick to the operator leaving traces on clothes. The aim of this study is to find the detection limits (sensitivity) to develop a screening device for civil applications (i.e., traces of explosive precursors on clothing to prevent terrorist attack in airports, malls, and public buildings). For this reason, in this work, four precursors (urea, sodium perchlorate, ammonium nitrate, and sodium nitrate) were chosen and detected over different colored textiles using UV Raman scattering. Usually, the amount of an explosive precursor left from a fingerprint is estimated to be in the order of micrograms ($\sim 10 \mu\text{g}$) and the chemical solid traces tend to adhere quite well on a rough surface.⁹ Raman spectroscopy allows low species concentration detection (traces) while the main experimental limit is the low intensity of the scattered radiation. The laser wavelength is chosen close to the electronic transition of a target molecule to be tested so that the inelastic scattered signal identifies a specific compound. For resonant Raman scattering, the scattered radiation carrying the signal information is inversely proportional to the forth power of the incident laser radiation wavelength, therefore,

*Address all correspondence to Emanuela Gallo, emanuela.gallo@dlr.de

an ultraviolet laser source was chosen since the signal increases several orders of magnitude when compared to the visible light. Furthermore, invisible light is suitable for covert detection applications.

2 Experimental Setup

2.1 Optical Setup

Figure 1 shows a sketch of the Raman laser and optical setup. A Continuum Sunlite EX-OPO FX-1 laser tunable source provided the 264 nm (10 Hz repetition rate, 3-ns pulse length, $<0.3 \text{ cm}^{-1}$ linewidth) excitation wavelength. The laser beam was relayed by several high UV reflective mirrors to the sample. The backscattered Raman signal was collected by a 12-cm parabolic UV mirror at 45 deg standing $\sim 60 \text{ cm}$ far from the sample and then sent through an optical fiber (600 μm resolution) connected to a Horiba iR550 spectrometer (2400 line/mm holographic grating, blaze 250 mm, 0.06 nm resolution, CCD 1024×256 -pixel, maximum resolution 0.01 nm). A 266 nm long-pass filter was placed in front of the fiber to reject the incoming UV laser radiation.

2.2 Samples Preparation

Explosive precursors samples were prepared over different colored textile materials: urea (Fig. 2), sodium perchlorate (Fig. 3), ammonium nitrate (Fig. 4), and sodium nitrate (Fig. 5). The preparation of the samples was a challenging task to provide realistic scenarios. A standard drop-cast method [REF] was not suitable because the solution tended to penetrate into textile without leaving all the traces on the surface. Another difficulty was due to the lab configuration:

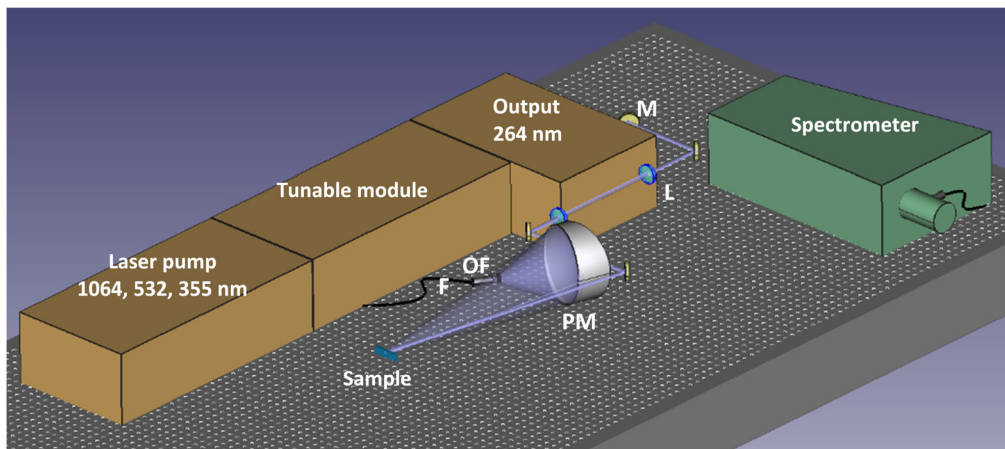


Fig. 1 Raman lab optical setup (M = mirror, L = lens, PM = parabolic mirror, F = fiber, OF = optical filter).

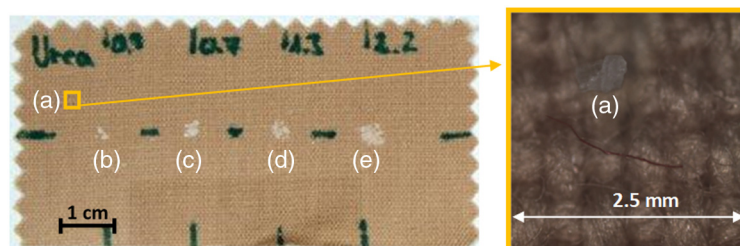


Fig. 2 Brown textile sample of urea at different nominal concentrations (a) traces (microscope image $\times 50$); (b) 0.25 mg; (c) 0.5 mg; (d) 1 mg; and (e) 2 mg.

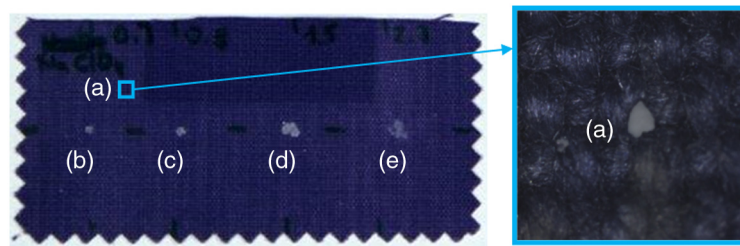


Fig. 3 Blue textile sample of sodium perchlorate at different nominal concentrations (a) traces (microscope image $\times 50$); (b) 0.25 mg; (c) 0.5 mg; (d) 1 mg; and (e) 2 mg.

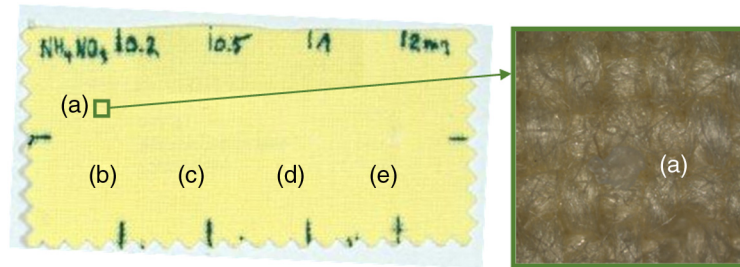


Fig. 4 Yellow textile sample of ammonium nitrate at different nominal concentrations (a) traces (microscope image $\times 50$); (b) 0.25 mg; (c) 0.5 mg; (d) 1 mg; and (e) 2 mg.

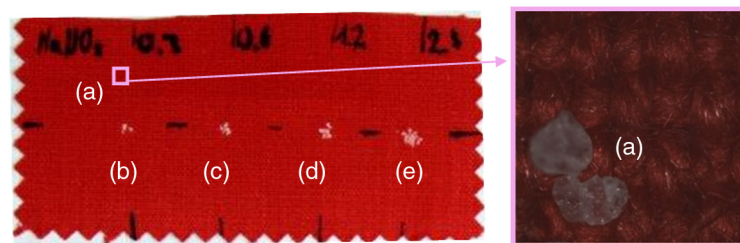


Fig. 5 Red textile sample of sodium nitrate at different nominal concentrations (a) traces (microscope image $\times 50$); (b) 0.25 mg; (c) 0.5 mg; (d) 1 mg; and (e) 2 mg.

the sample must stand vertically, hence the precursors' material must sustain gravity during the measurements. For this reason, a new method was employed: standardized amount of 2, 1, 0.5, and 0.25 mg and traces (μg range) for each respective precursor were first weighted and then pressed at 5 tons over colored cotton textiles. The applied method was found successful in both having the precursors' crystal on the textile surface and in having the sample standing. The sample areas were prepared to be below the upcoming laser beam size (elliptic shape $6\text{ mm} \times 3\text{ mm}$, 2 mJ per pulse, $14\text{ mJ}/\text{cm}^2$). All the samples were first analyzed to verify their distribution using an Olympus LEXT OLS 4000 3D microscope with a $50\times$ magnification. In addition, these images were used to quantify the overall amount of the sample over the background surface. Traces were photographed after all tests to observe a photo deterioration of the chemical compound or any possible background photobleaching.

2.3 Sample Image Analysis

For each precursor measurement, it was possible to quantify the amount probed. An arbitrary threshold was applied using ImageJ2 software¹⁰ to each microscope image to force each pixel to be either black or white as shown in Fig. 6. White indicates the presence of precursor crystal while black indicates its absence. Knowing the size of the picture ($2583 \times 2574\ \mu\text{m}$) and the percentage of white pixels, it was possible to calculate the area covered by each precursor.

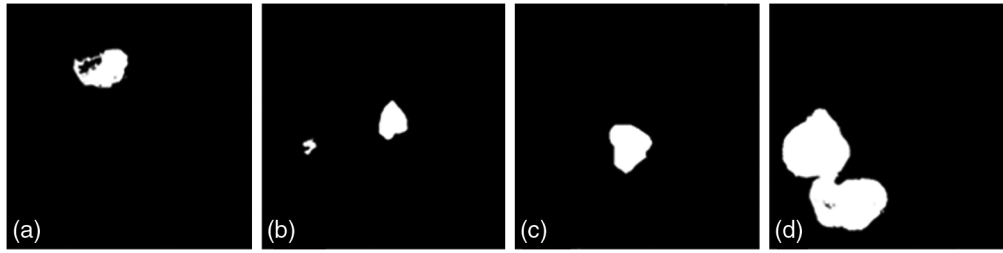


Fig. 6 Applied black and white threshold of microscope image 50 \times magnification of selected images of (a) urea; (b) sodium perchlorate; (c) ammonium nitrate; and (d) sodium nitrate.

Table 1 Effective measured amount in μg for all samples.

sample	nominal value mg	Urea μg	NaClO_4 μg	NH_4NO_3 μg	NaNO_3 μg
a.	traces	2.1	14.5	3.4	100.7
b.	0.25	12.8	263.3	7.2	180.4
c.	0.50	52.2	352.4	28.4	309.2
d.	1.00	58.9	382.3	32.3	421.6
e.	2.00	121.3	400.1	68.0	453.6

Then knowing from literature¹¹ the penetration depth and the respective given density, the effective amount measured was finally computed and summarized in Table 1. The penetration depth at 266 nm was found in literature for urea and ammonium nitrate (11 μm) while for sodium perchlorate and sodium nitrate the maximum penetration depth was assumed to be the depth crystal measured with the microscope (average 60 μm). From Table 1 It is possible to calculate the sensitivity of this experiment. The minimum effective amount measured on traces for all the tested explosive precursors was found to be: 2.1 μg for urea, 14.5 μg for sodium perchlorate, 3.4 μg for ammonium perchlorate, and 100.7 μg for sodium nitrate.

3 Results

3.1 Raman Spectra

Deep UV Raman spectra of the selected explosive precursors [urea (Fig. 8), sodium perchlorate (Fig. 9), ammonium nitrate (Fig. 10), and sodium nitrate (Fig. 11)] were detected over a remote

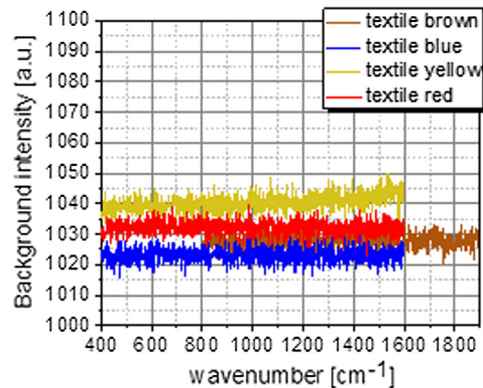


Fig. 7 Background of colored textiles (brow, blue, yellow, and red) recorded for 3 s.

distance of 60 centimeters. The overall testing time was 3 s for each experimental point (10 integrated nanosecond pulses acquired at 10 Hz, three accumulations). All spectra were background subtracted. The textile background signals were recorded at the same operating conditions and shown in Fig. 7. It can be noticed that Raman signal was not detected from the colored dyes used to change the fabric color. Therefore, it is not expected any interference due to peak overlap. A little bit of fluorescence is observed for the yellow color textile used (yellow curve). In this case, the observed effect was about 10 counts shift upward on the right between 1200 and 1600 cm^{-1} . However, this effect is neglectable comparing the Raman signal strength so no significant fluorescence interference is expected during the detection of the explosive precursors as well. In addition to the five different amounts of chemicals, a measurement of the bulk compound (labeled as f) is also provided for comparison. The bulk consisted in a 1 cm \times 1 cm standard chemical QS-Suprasil cuvette filled with each chemical respectively. Figure 8 shows the Raman spectra of urea. A distinct Raman peak simultaneously identifies several chemicals in a sample even if the spectral signatures seem closer. The strongest Raman vibrational ν_1 mode ($\text{NH}_2\text{-CO-NH}_2$ planar) for urea was detected at 1007 cm^{-1} .¹² This spectral line is chosen to be the specific signature for urea since it appears for all the concentrations. Above 0.5 mg, a secondary peak appears on the right-hand side of to the strongest one and it can be distinguished from the background (1172 cm^{-1} , $\text{NH}_2\text{-CO-NH}_2$ planar vibrational mode). For concentrations above 1 mg [Figs. 6(d) and 6(e)], three main peaks can be distinguished: 1465 cm^{-1} (asymmetric NCN stretch), 1536 cm^{-1} (NH_2 bend) and the close 1578, and 1646 cm^{-1} (CO stretch).¹² Figure 9 shows the Raman spectra of sodium perchlorate. A main Raman vibrational ν_1 mode (Cl-O symmetric stretch) at 948 cm^{-1} ¹³ can be noticed for all the concentrations tested. A secondary double peak (ν_3 antisymmetric stretch) at 1087 and 1148 cm^{-1} is distinguishable

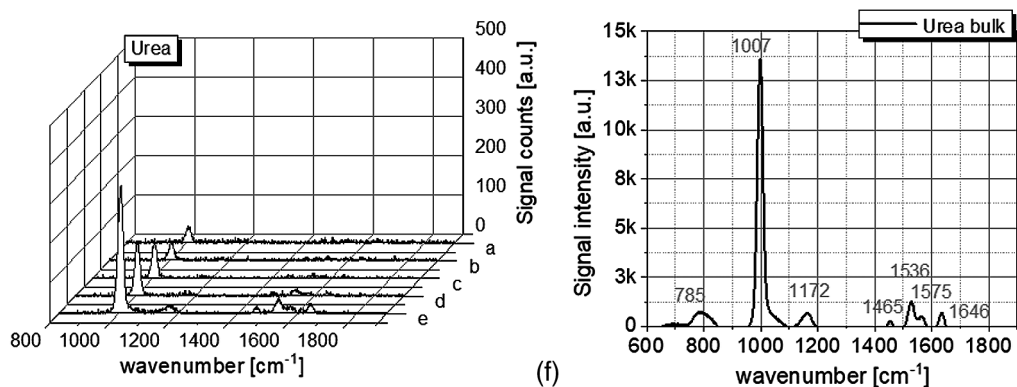


Fig. 8 UV Raman spectra probed from the urea sample of Fig. 2. at different concentration: (a) traces; (b) 0.25 mg; (c) 0.5 mg; (d) 1 mg; (e) 2 mg; and (f) pure.

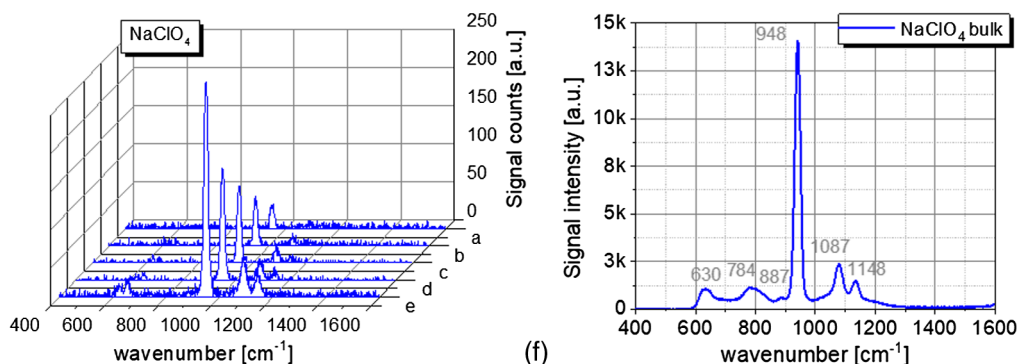


Fig. 9 UV Raman spectra probed from sodium perchlorate sample of Fig. 2. at different concentration: (a) traces; (b) 0.25 mg; (c) 0.5 mg; (d) 1 mg; (e) 2 mg; and (f) pure.

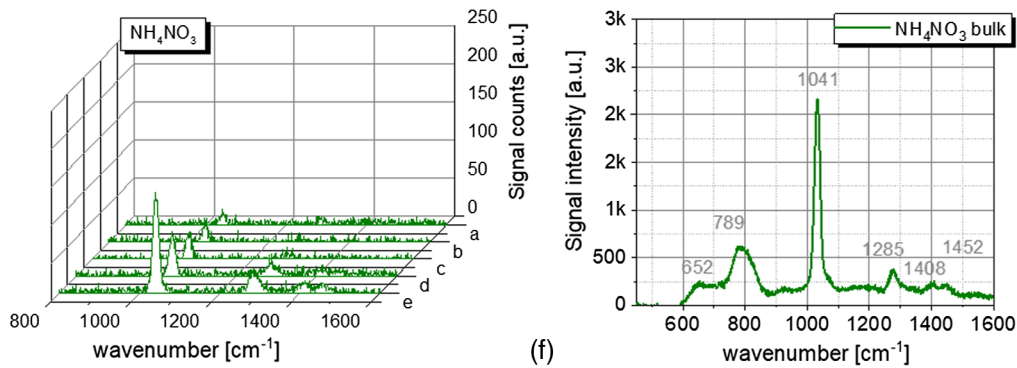


Fig. 10 UV Raman spectra probed from ammonium nitrate sample of Fig. 3. at different concentration: (a) traces; (b) 0.25 mg; (c) 0.5 mg; (d) 1 mg; (e) 2 mg; and (f) pure.

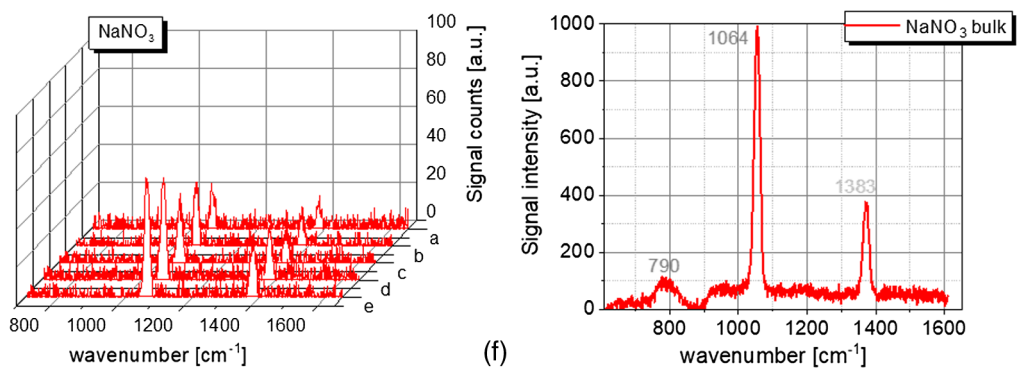


Fig. 11 UV Raman spectra probed from the sodium nitrate sample of Fig. 4. at different concentration: (a) traces; (b) 0.25 mg; (c) 0.5 mg; (d) 1 mg; (e) 2 mg; and (f) pure.

above 0.5 mg. A weak ν_4 (antisymmetric band) peak placed on the left-hand side of the strong ν_1 at 630 cm^{-1} is barely noticeable. Figure 10 shows the Raman spectra of ammonium nitrate. We notice a characteristic ν_1 band (symmetric stretch) at 1041 cm^{-1} for all the samples.⁶ Above 0.5 mg, some secondary vibrational modes appear respectively from left to right at 1285 cm^{-1} (ν_3), a double peak at 1408 and 1452 cm^{-1} . In the region between 1400 and 1500 cm^{-1} those vibrational modes are related to the NH_4 deformation and the NO_3 stretching.¹² Figure 11 shows the Raman spectra of sodium nitrate. For all the different amount probed, the two vibrational modes at 1064 cm^{-1} (ν_1)¹⁰ and 1383 cm^{-1} (ν_3) are always visible. The vibrational mode at 1668 cm^{-1} vanishes at the background noise level; however, both ν_1 and ν_3 bands can be used to clearly identify the presence of this precursor over the others. The stronger Raman signal recorded for traces was urea, followed by NaClO_4 , NH_4NO_3 , and NaNO_3 . As expected the bulk materials show the strongest signal-to-noise ratio (S/N) and the signal strength keeps decreasing lowering the amount of the chemicals. In all the recorded spectra, a significant interfering fluorescence was not observed and photo degradation was minimized keeping the average laser energy below 2 mJ per pulse. However, despite the laser energy was relatively low, it was not kept under the maximum permissible skin and eye exposure limits of 3 mJ/cm^2 (MPEs) for a nanosecond laser source.¹⁴ The eye-safe requirement would be an important target if the system will be employed in public spaces and it will be addressed in the near future.

3.2 Detection Limits

Figure 12 represents the S/N versus the effective mass amounts previously calculated from each explosive precursor in Table 1. For every sample tested, the S/N was calculated as $S/N = 2 \times H$ signal/h background.¹⁵ The value h background was calculated as the difference of maximum

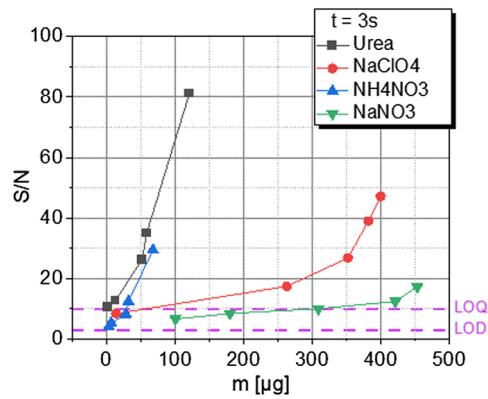


Fig. 12 Raman S/N over species concentration (a) urea; (b) ammonium nitrate; (c) sodium perchlorate; and (d) sodium nitrate. 3 s acquisition time.

and minimum value in a region without the presence of the Raman signal. Since every explosive precursor has a different Raman signature, it was not possible to choose a unique region to determine the background. For this reason, the range was chosen from 1220 to 1420 cm^{-1} for both urea and NaClO_4 , from 80 to 1000 cm^{-1} for NH_4NO_3 , and from 1120 to 1320 cm^{-1} for NaNO_3 . Figure 12 also shows the limit of detection (LOD) and the limit of quantification (LOQ) respectively defined as three times and ten times the S/N.¹⁵ It can be noticed that for all the cases S/N is >3 , so the detection is always possible for all precursors even in the smallest amounts. The LOQ shows that it is possible to quantify the acquired spectra for urea for the lowest masses measured. For the other precursors there are limitations: for sodium perchlorate, quantification is possible above 15 μg ; for ammonium nitrate, more than 30 μg are necessary; and for sodium nitrate, 200 μg are required due to its low signal intensity.

4 Conclusions

An experimental setup for a remote backscattering UV Raman spectroscopy was optimized for the investigation of precursors of explosives (urea, sodium perchlorate, ammonium nitrate, and sodium nitrate) on contaminated colored textile backgrounds within 3 s of acquisition time. First results were presented in this study to identify the detection limits for all the selected precursors. The measurements were performed over pressed (5 tons) standardized quantities of precursors on textiles. This method was found more reliable than the standard drop-casting. The exact detectable amount was then calculated using microscope images. The Raman signature of all the precursors was compared to the bulk measurement and corresponded to the signature of the bulk known from the literature. The minimum detectable amount was found to be: 2.1 μg for urea, 14.5 μg for sodium perchlorate, 3.4 μg for ammonium perchlorate, and 100.7 μg for sodium nitrate with exciting laser energy of 2 mJ/pulse. S/N and LOD were calculated and, for all the precursors, it is always possible to achieve a clear identification. Limits of quantification were also found to be: 2 μg for urea, 15 μg for sodium perchlorate, 30 μg for ammonium nitrate, and 200 μg for ammonium nitrate. Moreover, in the test performed, the choice of 264-nm laser excitation wavelength was found to be free from interfering fluorescence and photo-deterioration of the sample was not observed in the subsequent microscope imaging. A further optimization of the system will be performed to possibly decrease the detectable amount limits (maybe lowering the excitation wavelength toward deeper UV), the laser energy density (toward eye-safe), and increase detection distance.

Acknowledgments

The authors would like to thank Kirsten Klaffki for providing the microscope images and Björn Prietzel for the chemical laboratory help.

References

1. R. Chirico et al., "Proximal detection of traces of energetic materials with an eye-safe UV Raman prototype developed for civil applications," *Sensors* **16**, 8 (2016).
2. K. B. Mabrouk, T. H. Kauffmann, and M. D. Fontana, "Abilities of Raman sensor to probe pollutants in water," *J. Phys. Conf. Ser.* **450**, 012014 (2013).
3. S. Gulia et al., "Trace detection of explosive and their derivatives in stand-off mode using time gated Raman spectroscopy," *Vib. Spectrosc.* **87**, 207–214 (2016).
4. Committee on the Review of Existing and Potential Standoff Explosives Detection Techniques, "Existing and potential standoff explosives techniques," pp. 1–148, National Academies Press (2004).
5. A. Dogariu, "Standoff explosive detection and hyperspectral imaging using coherent anti-stokes Raman spectroscopy," in *Front. Opt.*, Optical Society of America, LTh4G.4 (2013).
6. R. L. Aggarwal et al., "Raman spectra and cross sections of ammonia, chlorine, hydrogen sulfide, phosgene, and sulfur dioxide toxic gases in the fingerprint region 400–1400 cm⁻¹," *AIP Adv.* **6**, 025310 (2016).
7. P. M. Pellegrino, E. L. Holthoff, and M. E. Farrell, *Laser-Based Optical Detection of Explosives*, CRC Press, Taylor & Francis Group, Boca Raton, Florida (2015).
8. "Regulation (EU) 98/2013 of the European Parliament and of the Council on the marketing and use of explosives precursors," 15 January 2013, <https://eur-lex.europa.eu/legal-content/EN/TXT/?uri=CELEX%3A32013R0098&qid=1629925675717>.
9. L. A. Skvortsov, "Laser methods for detecting explosive residues on surfaces of distant objects," *Quantum Electron.* **42**, 1 (2012).
10. C. T. Rueden et al., "ImageJ2: ImageJ for the next generation of scientific image data," *BMC Bioinf.* **18**(1), 529 (2017).
11. M. Amin et al., "Optimization of ultraviolet Raman spectroscopy for trace explosives checkpoint screening," *Anal. Bioanal. Chem.* **412**, 4495–4504 (2020).
12. T. E. Acosta-Maedar et al., "Remote Raman measurements of minerals, organics and inorganics at 430 m range," *Appl. Opt.* **55**, 10283–10289 (2016).
13. C. Ruan, W. Wang, and B. Gu, "Surface-enhanced Raman scattering for perchlorate detection using cystamine-modified gold nanoparticles," *Anal. Chem. Acta* **567**, 114–120 (2006).
14. S. Almaviva et al., "A new eye-safe UV Raman spectrometer for the remote detection of energetic materials in fingerprints concentrations: characterization by PCA and ROC analyzes," *Talanta* **144**, 420–426 (2015).
15. A. Shrivastava and V. B. Gupta, "Methods for the determination of limit of detection and limit of quantitation of the analytical methods," *Chron. Young Sci.* **2**(1), 21–25 (2011).

Emanuela Gallo is a current research scientist at the German Aerospace Center (DLR) and her research interests are in advanced lasers, optical detection systems, high speed and hot flows. Prior to working at DLR she was a research contractor at NASA LaRC. She received her PhD in aerospace engineering from George Washington University, her MS in aerospace engineering from Virginia Tech, and her BS in aerospace engineering from Polytechnic of Milan.

Luca Cantu is a research scientist at the German Aerospace Center (DLR). His work is mainly focused on the remote Raman detection of explosives and warfare agents. Previously, he was working in another branch of DLR working on laser thermometry in gas turbine combustion. He received his PhD from George Washington University in aerospace engineering, and in the same major obtained the MS from Virginia Tech and BS from Polytechnic of Milan.

Frank Duschek is the head of the atmospheric propagation and effect department (APW) of the Technical Physics Institute at the German Aerospace Center (DLR). He received his doctorate in chemistry from the University of Würzburg.